SPANDIDOS PUBLICATIONS

High-throughput DNA hypermethylation profiling in different ovarian epithelial cancer subtypes using universal bead array

MAN SOO YOON[1], DONG SOO SUH[1], KYUNG UN CHOI[2], MEE YOUNG SOL[2], DONG HOON SHIN[2], WON YOUNG PARK[2], JUNG HEE LEE[2], SEONG MUK JEONG[2], WOO GYEONG KIM[2] and NA RI SHIN[2]

Departments of [1]Obstetrics and Gynecology, [2]Pathology, Medical Research Institute, School of Medicine, Pusan National University, Gyeongsangnam-do 626-770, Republic of Korea

Received March 17, 2010; Accepted July 1, 2010

DOI: 10.3892/or_00000937

Abstract. DNA hypermethylation is common and plays a critical role in the regulation of gene expression. It is considered a major cause of carcinogenesis. High-throughput profiling method has been developed to analyze the methylation status of hundreds of pre-selected genes simultaneously. The aim of this study was to analyze promoter hypermethylation profiles of each subtype of ovarian epithelial cancer (OEC), to improve the understanding of the role of epigenetic silencing in carcinogenesis. DNA hypermethylation profiles on fresh frozen tissue samples of 5 serous, 3 mucinous, 5 endometrioid and 4 clear cell types of OEC, as well as 5 normal ovarian tissue samples as control. We used a high-throughput method for analyzing the hypermethylation status of 1,505 CpG loci selected from 871 genes simultaneously by GoldenGate Methylation Cancer Panel I (Illumina Human-6 v2 Expression BeadChip). Methylation status of seven genes was verified by methylation specific PCR (MSP). We identified 20, 37, 15 and 56 hypermethylated CpG locations in serous, mucinous, endometrioid and clear cell type OEC compared to control. Only 6 CpG loci were commonly hypermethylated across all subtypes of OEC. Hypermethylated loci of serous 17 (81.0%) and endometrioid type 10 (71.4%) were identical to that of clear cell type. However, mucinous type showed 17 peculiar loci (43.6%) out of 39 hypermethylated loci. The unique DNA hypermethylation patterns identified in different OEC subtypes suggest that their cause may involve different epigenetic mechanisms and the Bead chip used in this study is a useful tool to analyze DNA hypermethylation.

Introduction

Ovarian cancer is the fourth leading cause of cancer death in women (1). Patients (70%) have advanced disease (stage III or IV) upon presentation, with a 5-year survival between 15 and 20% at best with aggressive treatment. Ovarian epithelial cancer (OEC) accounts for over 90% of all cases and includes the following major histological subtypes: serous, mucinous, endometrioid and clear cell carcinomas. Cytogenetic and molecular analyses indicated that multiple genetic alterations were involved in the pathogenesis of ovarian cancer. *BRCA1* and *BRCA2* mutations are associated with increased ovarian cancer risks (2). Some studies have showed that *p16* loss was associated with ovarian cancer prognosis (3). However, it remains unclear how genetic alterations lead to development and subsequent progression of ovarian cancer. Better understanding of the molecular mechanisms responsible for ovarian cancer development and progression will improve diagnosis and treatment of this disease.

DNA methylation is an epigenetic alteration that plays an important role in carcinogenesis (4). The importance of aberrant CpG island methylation as an alternative mechanism to inactivate tumor suppressor genes has been recognized recently. Addition of a methyl group to the cytosine residues of CpG dinucleotide clusters in the 5' regulatory regions of genes occurs frequently in cancer cells, but seldom in non-malignant cells. Aberrant DNA methylation occurs at the cytosines of CpG dinucleotides, which often exist in clusters called CpG islands. When methylation of these sites occurs in the promoter region of a gene, it can result in gene silencing. Silencing of functionally important genes leads to a state of high cellular proliferation. Hypermethylated CpG islands play a causal role in promoting cancer development and are useful molecular markers for diagnosis and prognosis.

Aberrant promoter methylation has been associated with loss of expression of a growing number of tumor-related genes in a variety of human cancers (5-8). For example, aberrant DNA methylation is a frequent epigenetic event in ovarian cancer. The importance of the role of aberrant methylation in ovarian cancer has become increasingly apparent with a growing list of genes, such as *p16* (2,9), *BRCA1*, *HIC1*, *MLH1* and *RASSF1A* (2,10-15). Methylation frequencies were higher in OEC than in borderline ovarian tumors (9). Currently, relatively little is known about the specific patterns of CpG island hypermethylation in different subtypes of OEC (16).

A number of recent methodological advances in the investigation of DNA methylation have enhanced the analysis of the role methylation plays in cancer. The application of DNA

Correspondence to: Dr Kyung Un Choi, Department of Pathology, Pusan National University, Beomeo-ri, Mulgeum-eup, Yangsan-si, Gyeongsangnam-do 626-770, Republic of Korea
E-mail: kuchoi@pusan.ac.kr

Key words: hypermethylation, ovarian cancer, universal bead array

microarray technology has enabled the study of a large number of gene expression profiles from numerous tissue samples. It has provided an opportunity to classify different neoplasms based on characteristic expression patterns (17).

The GoldenGate genotyping assay was implemented on a BeadArray platform, a high throughout tool for studying methylation alterations, to determine the role of aberrant methylation in different OEC subtypes. The methylation status of 1,505 CpG sites in 871 genes was investigated in this study (18).

Materials and methods

Tissue and preparation of DNA samples. Normal and malignant ovarian tissue samples were obtained from the Pusan National University Hospital. Samples were stored at -70˚C. They included samples of fresh frozen tissue of 5 serous, 3 mucinous, 5 endometrioid and 4 clear cell type OEC. Histologic subtypes were determined according to World Health Organization (WHO) standards. Five normal ovarian tissue samples were used as control. Tissue samples were obtained from patients with advanced stage OEC (stage III, 9; stage IV, 8). Staging was performed according to the FIGO staging system. The mean age of patients was 55 years, and patient age ranged from 43 to 68 years. Genomic DNA was extracted from these specimens using the QIAamp tissue kit (Qiagen). Bisulfite-c verted DNA samples were prepared using the Zymo EZ DNA Methylation kit (Zymo Research). Bisulfite-converted DNA (5 μl) was mixed with 5 μl of photobiotin (MSI; Illumina) and incubated at 95˚C for 30 min.

Assay oligo extension and ligation. Biotinylated bisulfate-converted DNA was precipiated to remove free biotin, and subsequently dissolved biotinylated in solution (RS1; Illumina) bound to allele-specific oligonucleotides (ASOs) and locus-specific oligonucleotides (LSOs). Extension was carried out at 30˚C overnight. Master mix (37 μl) for extension and ligation (MEL; Illumina) was added to the extension products, and incubated for 15 min at 45˚C.

Polymerase chain reaction (PCR) amplification and PCR product preparation. After extension and ligation, beads were washed with universal buffer 1 (UB1; Illumina), re-suspended in 35 μl of elution buffer (IP1; Illumina) and heated at 95˚C for on 1 min to release ligated products. The supernatant was then used in a 60-μl PCR. PCR reactions were thermocycled as follows: 10 min at 37˚C, 3 min at 95˚C; 34 cycles (35 sec at 95˚C, 35 sec at 56˚C, 2 min at 72˚C); 10 min at 72˚C then cooled to 4˚C for 5 min. Three universal PCR primers (P1, P2 and P3) were respectively labeled with Cy3, Cy5 and biotin.

Double-stranded PCR products were immobilized on to paramagnetic particles by adding 20 μl of Paramagnetic Particle B Reagent (MPB; Illumina) to each 60 μl PCR, and incubated at room temperature for a minimum of 60 min. Bound PCR products were washed with universal buffer 2 (UB2; Illumina) and denatured by adding 30 μl of 0.1 N NaOH. After spending 1 min at room temperature, released single-stranded (ss) DNAs was neutralized with 30 μl of hybridization reagent (MH1; Illumina) and hybridized to arrays.

Array hybridization and imaging. Arrays were exposed to labeled ssDNA samples described above. Hybridization was performed under a controlled temperature gradient, from 60 to 45˚C over 12 h. Hybridization was held at 45˚C until the arrays were processed. After hybridization, the arrays were rinsed twice in UB2 and once with WC1 (WC1; Illumina) at room temperature, dried for 20 min, and then imaged at 0.8 μm resolution using a BeadArray Reader. Cy3 and Cy5 dyes were excited by laser emitted at 532 and 635 nm, respectively.

Methylation status was determinate by calculating ß, defined as the ratio of fluorescent signals of both methylated allele to the sum of the fluorescent signals of both methylated and unmethylated alleles. ß value ranged from 0 in the case of completely unmethylated sites to 1 in completely methylated sites. To identify hypermethylated sites, we applied an additional filter that required a minimum difference of 0.15 in ß between malignant and control samples.

Methylation specific polymerase chain reaction (MSP). The methylation status of 7 CpG island loci in malignant ovarian tissue samples and controls was determined by MSP. *DBC1*, *HOXA9*, *SCGB3A1*, *SPARC*, *SOX1*, *TWIST1* and *THY1* were selected for validation by MSP. DNA was extracted from 50 fresh frozen tissue samples of serous, mucinous, endometrioid, clear cell adenocarcinoma and normal ovarian tissue samples, using QIAamp DNA Micro kit (Qiagen, Hilden, Germany). Bisulfite treatment was carried out with 2 μg genomic DNA using EZ DNA Methylation Cold kit (Zymo Research) according to the manufacturer's protocol. DNA samples were then purified by the Wizard DNA Cliean-Up system (Promega, Madison, WI), then treated again with NaOH, ethanol-precipitated, and re-suspended in water.

For MSP, bisulfate-treated DNA samples were then used as PCR template with primers designed specifically for the CpG regions of each tested gene. Primer sequences of the methylated and unmethylated reaction were described in Table I. PCR mixture contained 2.5 μl of 10X PCR buffer, 1.0 μl of each primer, 2.5 μl of 2.5 mM dNTP and 0.2 μl (1 U) hot start Taq polymerase (Takara) in a final reaction volume of 25 μl. PCR products were electrophoresed on 2.5% agarose gel, stained with ethium bromide, and visualized under UV illumination.

A methylation-positive DNA control was prepared *in vitro* using SssI methylase (New England Biolabs, Beverly, MA), which methylated every cytosine of CpG dinucleotide in the DNA. Ten samples of non-malignant ovarian tissue were selected as control.

Results

Global methylation profiles in OECs. We measured the methylation status of the 1,505 CpG sites from 871 genes in different types of OECs, including serous, mucinous, endometrioid, and clear cell adenocarcinoma, and normal ovarian tissue samples as control. From this study, we obtained a list of differentially methylated markers that distinguished malignant from normal tissue samples. We identified 20, 37, 15 and 56 hypermethylated CpG sites from 19, 33, 14 and 46 genes in respectively serous, mucinous, endometrioid and

MSP primer sequence, product size and annealing temperature.

Gene	Primer	Product size (bp)	Annealing temperature (˚C)
DBC1			
Mf	5'-TAGAGAGATGTGTAGATATAAATGG-3'	269	57
Mr	5'-CCCAAATAAACTAAAACTAAACCATA-3'		
Uf	5'-ATAGAGAGACGCGTAGATATAAACG-3'	269	55
Ur	5'-CCGAATAAACTAAAACTAAACCGTA-3'		
HOXA9			
Mf	5'-GGTTAATGGGGGCGCGGGCGT-3'	127	66
Mr	5'-AACGCCTAACCCGCCCGACCC-3'		
Uf	5'-GTATGGTTAATGGGGGTGTGGGTGT-3'	139	66
Ur	5'-CCATACCCAACACCTAACCCACCCAACCC-3'		
SCGB3A1			
Mf	5'-GGTACGGGTTTTTTACGGTTCGT-3'	135	57
Mr	5'-AACTTCTTATACCCGATCCTC-3'		
Uf	5'-GGTATGGGTTTTTTATGGTTTGT-3'	138	57
Ur	5'-CAAAACTTCTTATACCCAATCCTC-3'		
SPARC			
Mf	5'-GAGAGCGCGTTTTGTTTGTC-3'	112	62
Mr	5'-AACGACGTAAACGAAAATATCG-3'		
Uf	5'-TTTTTTAGATTGTTTGGAGAGTG-3'	132	62
Ur	5'-AACTAACAACATAAACAAAAATATC-3'		
SOX1			
Mf	5'-CGTTTTTTTTTTTTCGTTATTGGC-3'	135	62
Mr	5'-CCTACGCTCGATCCTCAACG-3'		
Uf	5'-TGTTTTTTTTTTTTTGTTATTGGTG-3'	135	56
Ur	5'-CCTACACTCAATCCTCAACAAC-3'		
TWIST1			
Mf	5'-TTTCGGATGGGGTTGTTATC-3'	200	55
Mr	5'-AAACGACCTAACCCGAACG-3'		
Uf	5'-TTTGGATGGGGTTGTTATTGT-3'	193	55
Ur	5'-CCTAACCCAAACAACCAACC-3'		
THY1			
Mf	5'-TATTTTTATATTAATGCGGGATCGT-3'	172	53
Mr	5'-CGATTACTACACCCAACTCGAA-3'		
Uf	5'-TTATTTTTATATTAATGTGGGATTGT-3'	175	50
Ur	5'-TCCAATTACTACACCCAACTCAAA-3'		

clear cell OEC subtype, which showed higher ß values (≥0.6) compared to that of normal ovarian tissue (≤0.4). Only 6 CpG loci were commonly hypermethylated across all types of OEC; *ALOX12*, *DAB2IP*, *HOXA9*, *HOXA11*, *MOS* and *SPARC*. Hypermethylated loci in serous 17 (81.0%) and endometrioid subtypes 10 (71.4%) were in common with that of clear cell subtype. However, the mucinous subtype showed 17 peculiar loci (43.6%) out of 39 hypermethylated loci. Selected genes fall into various classes, including tumor suppressor genes and genes involved in apoptosis, DNA repair, cell cycle, cell proliferation, differentiation, development, cell signaling, cell adhesion, transcription regulation and angiogenesis. Figs. 1 and 2 illustrate differential methylation profiles in malignant and control tissue samples, as well as specific methylation signatures obtained for individual OEC subtype.

Validation of array results by MSP. We used MSP to confirm methylation status of the CpG sites of 7 genes identified by our microarray analysis; *HOXA9*, *SPARC*, *SOX1*, *DBC1*, *TWIST1*, *SCGB3A1* and *THY1* (Fig. 3).

HOXA9 and *SPARC* were hypermethylated in all OEC subtypes and were selected for validation. They were hypermethylated in relatively high frequencies (22/40, 55% and 11/40, 27.5%). *SOX1* promoter hypermethylation observed in all OECs except the endometrioid subtype on microarray was detected in 12 OEC tissue samples (30%). Only one endometrioid adenocarcinoma tissue sample was confirmed *SOX1* hypermethylation on MSP. Hypermethylated *DBC1* and *TWIST1* demonstrated only in mucinous adenocarcinoma were evaluated by MSP. Mucinous adenocarcinoma showed more promoter hypermethylation in two genes compared to other OEC subtypes. Promoter hypermethylation in *DBC1* and *TWIST1* were detected in respectively 4 (40%) and 2 (20%) mucinous adenocarcinoma samples. In contrast, *DBC1* hypermethylation was detected in only 13.3% (4/30) of the other OEC subtypes. Particularly, no hypermethylation was observed in other OEC subtypes for *TWIST1*. Four clear cell adenocarcinomas samples (40%) showed *SCGB3A1* hypermethylation, and only one serous adenocarcinoma (10%) showed *SCGB3A1* hypermethylation. MSP identified *THY1* hypermethylation in 1 serous (10%), 1 mucinous (10%) and 3 clear cell adenocarcinomas (30%) tissue samples, but not in mucinous adenocarcinoma.

All of OEC tissue samples were found to have hypermethylation in one or more of the 7 genes of interest. Normal ovarian samples were unmethylated at these sites (Table II).

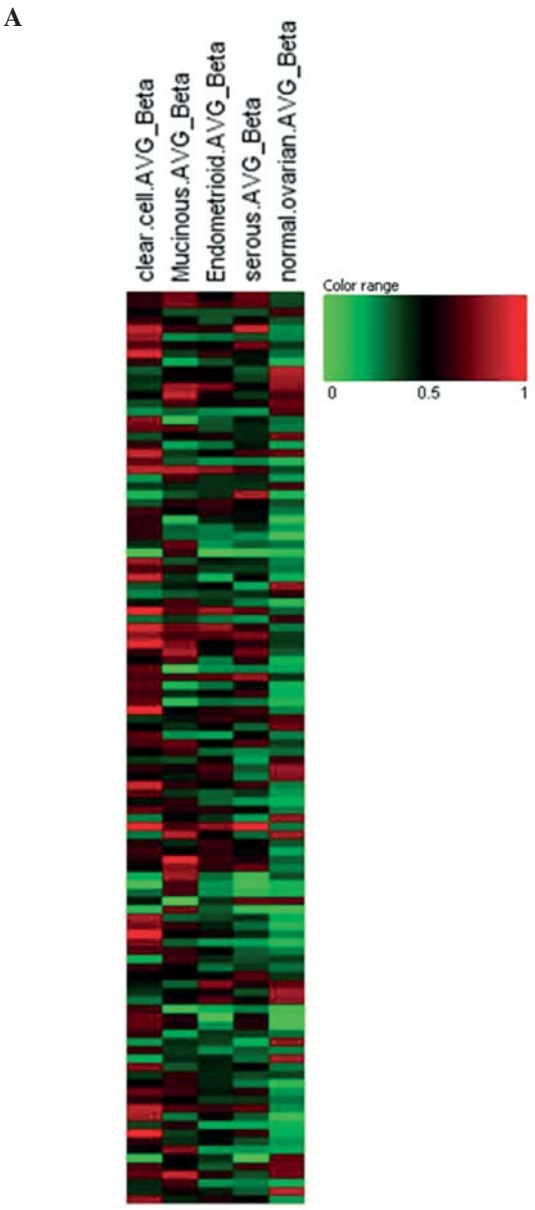

Figure 1. (A) Methylation profiling heat map feature of different types of epithelial ovarian cancers (EOCs).

Discussion

This study utilized a high-throughput methodology to analyze the methylation status of hundreds of genes simultaneously, in order to elucidate methylation signatures that distinguish malignant from normal ovarian tissue samples. We used universal bead array methylation profiles (GoldenGate Methylation Cancer Panel I; Illumina Human-6 v2 Expression BeadChip) of 1,505 CpG sites from 871 genes in a panel of different types of OEC. Bead array-based platform has recently been adapted to detect DNA methylation (18). The GoldenGate Methylation assay on a bead array platform retains the high sample throughput (up to 96 samples) provided by bisulfate-based techniques, but greatly expands the number of loci (up to 1,505 CpG sites) that can be interrogated simultaneously. This method can detect changes in methylation status with only 200 ng of genomic DNA. It does not simply measure DNA methylation qualitatively (positive vs. negative methylation), but a quantitative measure of DNA methylation levels. In this study, 22 OEC and normal ovarian tissue samples were simultaneously analyzed. We showed that CpG island hypermethylation is widespread in OEC genomes, and various hypermethylation patterns present in the different OEC subtypes.

Differential methylation was independently confirmed by MSP, yielding a select group of CpG loci that have previously been reported in OEC and other types of cancer, which may be useful as epigenetic markers for OEC. We also observed high concordance between results obtained by our microarray-based methylation analyses and that by MSP. These results led us to conclude that bead array methylation assay is appropriate for large-scale analyses of hypermethylated loci throughout the genome, whereas MSP is more sensitive in identifying a hypermethylated CpG locus at a time. As such, bead array methylation assay and MSP data did not completely correlate. This microarray-based technology can be considered a powerful method to simultaneously assess the methylation status of hundreds of genes in large populations.

In this study, numerous CpG loci were identified and the involving genes fall into various classes, including tumor suppressor genes and genes involved in apoptosis, DNA repair, cell cycle, cell proliferation, differentiation, development, cell signaling, cell adhesion, transcription regulation and angiogenesis. Some have previously been reported to be hypermethylated in OEC, including *APC* (11), *HOXA9* (19), *HOXA11* (20), *MYOD1* (21), *RASSF1* (22) and *SCGB3A* (19).

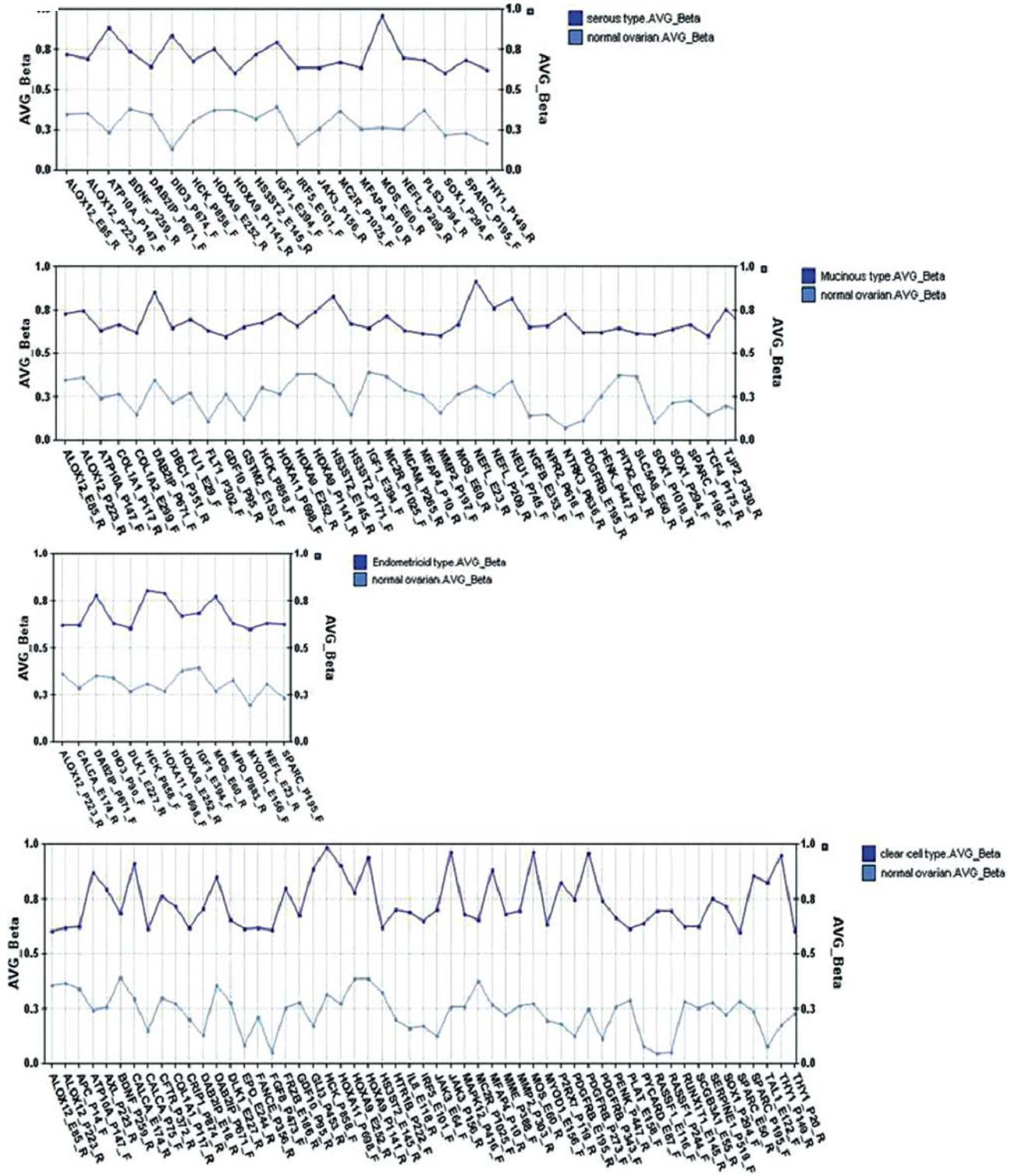

Figure 1. (B) Plot images of ß values.

Although homeobox genes have been studied extensively and their expression profiles determined in a number of human tissues, little is known about their methylation patterns, in both normal and malignant tissues. In this study, the promoter of *HOXA9* was frequently hypermethylated in all types of OEC. High *HOXA9* methylation frequency has been reported in all types of OEC (19). Therefore, aberrant gene expression of HOXA9 may be involved in ovarian carcinogenesis.

Secreted protein, acidic and rich in cysteine (SPARC) is a 35-kDa calcium binding glycoprotein involved in cell adhesion, motility and interactions with extracellular matrix components. SPARC expression and *SPARC* gene functional analysis in malignant tissues have been widely studied. Recent

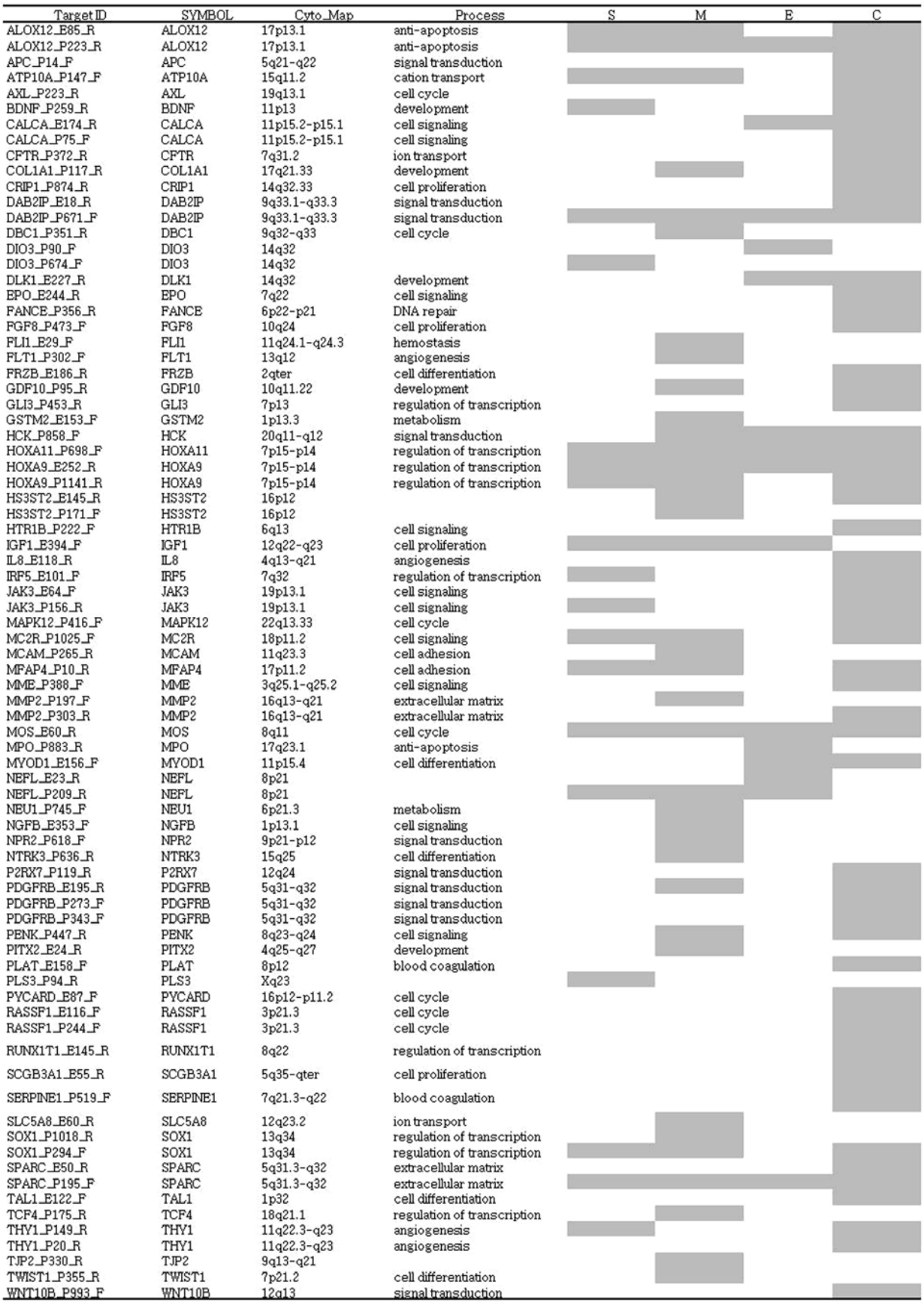

Target ID	SYMBOL	Cyto_Map	Process	S	M	B	C
ALOX12_E85_R	ALOX12	17p13.1	anti-apoptosis				
ALOX12_P223_R	ALOX12	17p13.1	anti-apoptosis				
APC_P14_F	APC	5q21-q22	signal transduction				
ATP10A_P147_F	ATP10A	15q11.2	cation transport				
AXL_P223_R	AXL	19q13.1	cell cycle				
BDNF_P259_R	BDNF	11p13	development				
CALCA_E174_R	CALCA	11p15.2-p15.1	cell signaling				
CALCA_P75_F	CALCA	11p15.2-p15.1	cell signaling				
CFTR_P372_R	CFTR	7q31.2	ion transport				
COL1A1_P117_R	COL1A1	17q21.33	development				
CRIP1_P874_R	CRIP1	14q32.33	cell proliferation				
DAB2IP_E18_R	DAB2IP	9q33.1-q33.3	signal transduction				
DAB2IP_P671_F	DAB2IP	9q33.1-q33.3	signal transduction				
DBC1_P351_R	DBC1	9q32-q33	cell cycle				
DIO3_P90_F	DIO3	14q32					
DIO3_P674_F	DIO3	14q32					
DLK1_E227_R	DLK1	14q32	development				
EPO_E244_R	EPO	7q22	cell signaling				
FANCE_P356_R	FANCE	6p22-p21	DNA repair				
FGF8_P473_F	FGF8	10q24	cell proliferation				
FLI1_E29_F	FLI1	11q24.1-q24.3	hemostasis				
FLT1_P302_F	FLT1	13q12	angiogenesis				
FRZB_E186_R	FRZB	2qter	cell differentiation				
GDF10_P95_R	GDF10	10q11.22	development				
GLI3_P453_R	GLI3	7p13	regulation of transcription				
GSTM2_E153_F	GSTM2	1p13.3	metabolism				
HCK_P858_F	HCK	20q11-q12	signal transduction				
HOXA11_P698_F	HOXA11	7p15-p14	regulation of transcription				
HOXA9_E252_R	HOXA9	7p15-p14	regulation of transcription				
HOXA9_P1141_R	HOXA9	7p15-p14	regulation of transcription				
HS3ST2_E145_R	HS3ST2	16p12					
HS3ST2_P171_F	HS3ST2	16p12					
HTR1B_P222_F	HTR1B	6q13	cell signaling				
IGF1_E394_F	IGF1	12q22-q23	cell proliferation				
IL8_E118_R	IL8	4q13-q21	angiogenesis				
IRF5_E101_F	IRF5	7q32	regulation of transcription				
JAK3_E64_F	JAK3	19p13.1	cell signaling				
JAK3_P156_R	JAK3	19p13.1	cell signaling				
MAPK12_P416_F	MAPK12	22q13.33	cell cycle				
MC2R_P1025_F	MC2R	18p11.2	cell signaling				
MCAM_P265_R	MCAM	11q23.3	cell adhesion				
MFAP4_P10_R	MFAP4	17p11.2	cell adhesion				
MME_P388_F	MME	3q25.1-q25.2	cell signaling				
MMP2_P197_F	MMP2	16q13-q21	extracellular matrix				
MMP2_P303_R	MMP2	16q13-q21	extracellular matrix				
MOS_E60_R	MOS	8q11	cell cycle				
MPO_P883_R	MPO	17q23.1	anti-apoptosis				
MYOD1_E156_F	MYOD1	11p15.4	cell differentiation				
NEFL_E23_R	NEFL	8p21					
NEFL_P209_R	NEFL	8p21					
NEU1_P745_F	NEU1	6p21.3	metabolism				
NGFB_E353_F	NGFB	1p13.1	cell signaling				
NPR2_P618_F	NPR2	9p21-p12	signal transduction				
NTRK3_P636_R	NTRK3	15q25	cell differentiation				
P2RX7_P119_R	P2RX7	12q24	signal transduction				
PDGFRB_E195_R	PDGFRB	5q31-q32	signal transduction				
PDGFRB_P273_F	PDGFRB	5q31-q32	signal transduction				
PDGFRB_P343_F	PDGFRB	5q31-q32	signal transduction				
PENK_P447_R	PENK	8q23-q24	cell signaling				
PITX2_E24_R	PITX2	4q25-q27	development				
PLAT_E158_F	PLAT	8p12	blood coagulation				
PLS3_P94_R	PLS3	Xq23					
PYCARD_E87_F	PYCARD	16p12-p11.2	cell cycle				
RASSF1_E116_F	RASSF1	3p21.3	cell cycle				
RASSF1_P244_F	RASSF1	3p21.3	cell cycle				
RUNX1T1_E145_R	RUNX1T1	8q22	regulation of transcription				
SCGB3A1_E55_R	SCGB3A1	5q35-qter	cell proliferation				
SERPINE1_P519_F	SERPINE1	7q21.3-q22	blood coagulation				
SLC5A8_E60_R	SLC5A8	12q23.2	ion transport				
SOX1_P1018_R	SOX1	13q34	regulation of transcription				
SOX1_P294_F	SOX1	13q34	regulation of transcription				
SPARC_E50_R	SPARC	5q31.3-q32	extracellular matrix				
SPARC_P195_F	SPARC	5q31.3-q32	extracellular matrix				
TAL1_E122_F	TAL1	1p32	cell differentiation				
TCF4_P175_R	TCF4	18q21.1	regulation of transcription				
THY1_P149_R	THY1	11q22.3-q23	angiogenesis				
THY1_P20_R	THY1	11q22.3-q23	angiogenesis				
TJP2_P330_R	TJP2	9q13-q21					
TWIST1_P355_R	TWIST1	7p21.2	cell differentiation				
WNT10B_P993_F	WNT10B	12q13	signal transduction				

Figure 2. Methylation status of epithelial ovarian cancers (EOCs).

reports highlighted the role of this molecule as positive and negative modulators in the pathogenesis of different malignancies (23). In many cancers, up-regulation of *SPARC* has been reported in the peri-tumoral stromal cells of prostate,

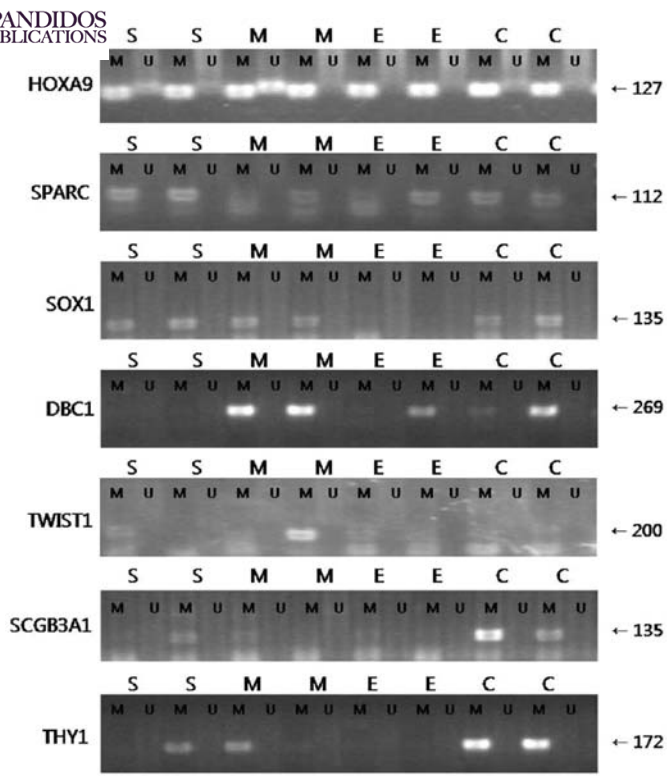

Figure 3. Representative methylation-specific polymerase chain reaction (MSP) results are shown for the 7 analyzed genes.

breast and esophageal cancer, as well as glioma (23,24). However, *SPARC* was down-regulated in some cancers, such as colorectal carcinomas (25). Down-regulation of *SPARC* is related to aberrant methylation of CpG islands in the promoter region. Ovarian cancer cells treated with SPARC showed inhibition of cell proliferation and underwent apoptosis (26). SPARC promoter hypermethylation was found in certain OEC subtypes in this study.

SCGB3A1, also named *HIN1* (high in normal-1), encodes a small secreted protein, secretoglobin 3A1 and belongs to the secretoglobin family. It is reported to be a potent inhibitor of anchorage-dependent and anchorage-independent cell growth, cell migration and invasion (27). Hypermethylation-induced down-regulation of this gene has been found in several cancer types, such as breast, lung, colorectal and testicular cancer, suggestive of tumor suppressor function (28). *SCGB3A1* hypermethylation has been reported in mucinous and clear cell adenocarcinoma subtypes (19). This study has also demonstrated that *SCGB3A1* promoter hypermethylation occurs in OECs, suggesting that this event plays a role in the development of certain OEC subgroup.

SOX1 is crucial for neuronal development. It has been reported that *SOX1* expression attenuates carcinogenic potential of neuronal precursors after neural stem cell transplantation (29). A recent study of DNA methylation using microarray in cervical cancer showed that *SOX1* was frequently hypermethylated in squamous cell carcinoma (30). We found that *SOX1* hypermethylation might be associated with OEC.

THY1 is a 25- to 28-kDa surface glycoprotein, which is expressed on the cytoplasmic membrane in different cell types (31). *THY1* triggers a variety of cellular functions, including proliferation, lymphokine release, differentiation and apoptosis. Despite extensive investigations, the exact function and physiologic role of *THY1* in the cell remains unknown (32). *THY1* is associated with tumor suppression in human ovarian cancer. However, there is a lack of direct evidence in support of *THY1* as a candidate tumor suppressor gene in ovarian cancer (32). A recent study showed that *THY1* was a good candidate tumor suppressor gene and the mechanism of *THY1* gene inactivation was attributed to hypermethylation in nasopharyngeal carcinoma (33). We suggest that *THY1* may be a candidate marker in ovarian carcinogenesis.

The deleted in bladder cancer 1 gene (*DBC1*) has been identified as a potential tumor suppressor gene commonly hypermethylated or deleted in bladder cancer (34). Abnormal methylation or deletion of *DBC1* has also been described in other cancers, such as oral squamous cell carcinoma and non-small cell lung cancer (35,36). *Twist* belongs to the basic-helix-loop-helix family of transcription factors and is implicated in lineage-specific cellular differentiation and survival (37). *TWIST1*, an anti-apoptotic and pro-metastatic transcription factor, is overexpressed in many epithelial cancers such as breast cancer (37). Recently, human breast carcinomas have been reported to exhibit *TWIST1* promoter hyper-

Table II. Summary of gene hypermethylation validated by MSP in EOCs.

Type of OEC	*HOXA9* (%)	*SPARC* (%)	*SOX1* (%)	*DBC1* (%)	*TWIST1* (%)	*SCGB3A1* (%)	*THY1* (%)
Serous (n=10)	7 (70)	3 (30)	4 (40)	1 (10)	0 (0)	1 (10)	1 (10)
Mucinous (n=10)	5 (50)	2 (20)	3 (30)	4 (40)	2 (20)	0 (0)	1 (10)
Endometrioid (n=10)	4 (40)	3 (30)	1 (10)	1 (10)	0 (0)	0 (0)	0 (0)
Clear cell (n=10)	6 (60)	3 (30)	4 (40)	2 (20)	0 (0)	4 (40)	3 (30)
Total (n=40)	22 (55)	11 (27.5)	12 (30)	8 (20)	2 (5)	5 (12.5)	5 (12.5)

methylation at high frequency, and methylation of the *TWIST1* promoter is a good predictor of human breast cancer (38). *DBC1* and *TWIST1* were hypermethylated predominantly in ovarian mucinous adenocarcinoma in this study, and therefore potentially a candidate marker of this OEC subtype.

This study has elucidated the importance of epigenetic regulation in the development of different OEC subtypes. We identified several epigenetically dysregulated gene targets in OEC through global screening, using a microarray-based assay and a subsequent validation method.

Acknowledgements

This work was supported by a grant of Medical Research Institute, Pusan National University, Busan, Republic of Korea (20080031000), and by a grant from the National R&D Program for Cancer Control, Ministry for Health, Welfare and Family Affairs, Republic of Korea (0920050).

References

1. Jemal A, Murray T, Ward E, Samuels A, Tiwari RC, Ghafoor A, Feuer EJ and Thun MJ: Cancer statistics, 2005. CA Cancer J Clin 55: 10-30, 2005.
2. Ibanez de Caceres I, Battagli C, Esteller M, Herman JG, Dulaimi E, Edelson MI, Bergman C, Ehya H, Eisenberg BL and Cairns P: Tumor cell-specific BRCA1 and RASSF1A hypermethylation in serum, plasma and peritoneal fluid from ovarian cancer patients. Cancer Res 64: 6476-6481, 2004.
3. Khouja MH, Baekelandt M, Nesland JM and Holm R: The clinical importance of ki-67, p16, p14 and p57 expression in patients with advanced ovarian carcinoma. Int J Gynecol Pathol 26: 418-425, 2007.
4. Esteller M, Corn PG, Baylin SB and Herman JG: A gene hypermethylation profile of human cancer. Cancer Res 61: 3225-3229, 2001.
5. Al-Kuraya K, Narayanappa R, Siraj AK, Al-Dayel F, Ezzat A, El Solh H, Al-Jommah N, Sauter G and Simon R: High frequency and strong prognostic relevance of O6-methylguanine DNA methyltransferase silencing in diffuse large B-cell lymphomas from the middle east. Hum Pathol 37: 742-748, 2006.
6. Chu LC, Eberhart CG, Grossman SA and Herman JG: Epigenetic silencing of multiple genes in primary CNS lymphoma. Int J Cancer 119: 2487-2491, 2006.
7. Gu J, Berman D, Lu C, Wistuba II, Roth JA, Frazier M, Spitz MR and Wu X: Aberrant promoter methylation profile and association with survival in patients with non-small cell lung cancer. Clin Cancer Res 12: 7329-7338, 2006.
8. Yang HJ, Liu VW, Wang Y, Tsang PC and Ngan HY: Differential DNA methylation profiles in gynecological cancers and correlation with clinico-pathological data. BMC Cancer 6: 212, 2006.
9. Wiley A, Katsaros D, Chen H, Rigault de la Longrais IA, Beeghly A, Puopolo M, Singal R, Zhang Y, Amoako A, Zelterman D and Yu H: Aberrant promoter methylation of multiple genes in malignant ovarian tumors and in ovarian tumors with low malignant potential. Cancer 107: 299-308, 2006.
10. Katsaros D, Cho W, Singal R, Fracchioli S, Rigault de la Longrais IA, Arisio R, Massobrio M, Smith M, Zheng W, Glass J and Yu H: Methylation of tumor suppressor gene p16 and prognosis of epithelial ovarian cancer. Gynecol Oncol 94: 685-692, 2004.
11. Makarla PB, Saboorian MH, Ashfaq R, Toyooka KO, Toyooka S, Minna JD, Gazdar AF and Schorge JO: Promoter hypermethylation profile of ovarian epithelial neoplasms. Clin Cancer Res 11: 5365-5369, 2005.
12. Rathi A, Virmani AK, Schorge JO, Elias KJ, Maruyama R, Minna JD, Mok SC, Girard L, Fishman DA and Gazdar AF: Methylation profiles of sporadic ovarian tumors and nonmalignant ovaries from high-risk women. Clin Cancer Res 8: 3324-3331, 2002.
13. Strathdee G, Appleton K, Illand M, Millan DW, Sargent J, Paul J and Brown R: Primary ovarian carcinomas display multiple methylator phenotypes involving known tumor suppressor genes. Am J Pathol 158: 1121-1127, 2001.
14. Teodoridis JM, Hall J, Marsh S, Kannall HD, Smyth C, Curto J, Siddiqui N, Gabra H, McLeod HL, Strathdee G and Brown R: CpG island methylation of DNA damage response genes in advanced ovarian cancer. Cancer Res 65: 8961-8967, 2005.
15. Huang YW, Jansen RA, Fabbri E, Potter D, Liyanarachchi S, Chan MW, Liu JC, Crijns AP, Brown R, Nephew KP, van der Zee AG, Cohn DE, Yan PS, Huang TH and Lin HJ: Identification of candidate epigenetic biomarkers for ovarian cancer detection. Oncol Rep 22: 853-861, 2009.
16. Santin AD, Zhan F, Cane' S, Bellone S, Palmieri M, Thomas M, Burnett A, Roman JJ, Cannon MJ, Shaughnessy J Jr and Pecorelli S: Gene expression fingerprint of uterine serous papillary carcinoma: identification of novel molecular markers for uterine serous cancer diagnosis and therapy. Br J Cancer 92: 1561-1573, 2005.
17. Wei SH, Chen CM, Strathdee G, Harnsomburana J, Shyu CR, Rahmatpanah F, Shi H, Ng SW, Yan PS, Nephew KP, Brown R and Huang TH: Methylation microarray analysis of late-stage ovarian carcinomas distinguishes progression-free survival in patients and identifies candidate epigenetic markers. Clin Cancer Res 8: 2246-2252, 2002.
18. Bibikova M, Lin Z, Zhou L, Chudin E, Garcia EW, Wu B, Doucet D, Thomas NJ, Wang Y, Vollmer E, Goldmann T, Seifart C, Jiang W, Barker DL, Chee MS, Floros J and Fan JB: High-throughput DNA methylation profiling using universal bead arrays. Genome Res 16: 383-393, 2006.
19. Wu Q, Lothe RA, Ahlquist T, Silins I, Tropé CG, Micci F, Nesland JM, Suo Z and Lind GE: DNA methylation profiling of ovarian carcinomas and their in vitro models identifies HOXA9, HOXB5, SCGB3A1 and CRABP1 as novel targets. Mol Cancer 6: 45, 2007.
20. Fiegl H, Windbichler G, Mueller-Holzner E, Goebel G, Lechner M, Jacobs IJ and Widschwendter M: HOXA11 DNA methylation - a novel prognostic biomarker in ovarian cancer. Int J Cancer 123: 725-729, 2008.
21. Cheng P, Schmutte C, Cofer KF, Felix JC, Yu MC and Dubeau L: Alterations in DNA methylation are early, but not initial, events in ovarian tumorigenesis. Br J Cancer 75: 396-402, 1997.
22. Choi YL, Kang SY, Choi JS, Kim SH, Lee SJ, Bae DS and Ahn G: Aberrant hypermethylation of RASSF1A promoter in ovarian borderline tumors and carcinomas. Virchows Arch 448: 331-336, 2006.
23. Porte H, Chastre E, Prevot S, Nordlinger B, Empereur S, Basset P, Chambon P and Gespach C: Neoplastic progression of human colorectal cancer is associated with overexpression of the stromelysin-3 and BM-40/SPARC genes. Int J Cancer 64: 70-75, 1995.
24. Le Bail B, Faouzi S, Boussarie L, Guirouilh J, Blanc JF, Carles J, Bioulac-Sage P, Balabaud C, Rosenbaum J: Osteonectin/SPARC is overexpressed in human hepatocellular carcinoma. J Pathol 189: 46-52, 1999.
25. Yang E, Kang HJ, Koh KH, Rhee H, Kim NK and Kim H: Frequent inactivation of SPARC by promoter hypermethylation in colon cancers. Int J Cancer 121: 567-575, 2007.
26. Yiu GK, Chan WY, Ng SW, Chan PS, Cheung KK, Berkowitz RS and Mok SC: SPARC (secreted protein acidic and rich in cysteine) induces apoptosis in ovarian cancer cells. Am J Pathol 159: 609-622, 2001.
27. Krop I, Parker MT, Bloushtain-Qimron N, Porter D, Gelman R, Sasaki H, Maurer M, Terry MB, Parsons R and Polyak K: HIN-1, an inhibitor of cell growth, invasion and AKT activation. Cancer Res 65: 9659-9669, 2005.
28. Shigematsu H, Suzuki M, Takahashi T, Miyajima K, Toyooka S, Shivapurkar N, Tomlinson GE, Mastrangelo D, Pass HI, Brambilla E, Sathyanarayana UG, Czerniak B, Fujisawa T, Shimizu N and Gazdar AF: Aberrant methylation of HIN-1 (high in normal-1) is a frequent event in many human malignancies. Int J Cancer 113: 600-604, 2005.
29. Fukuda H, Takahashi J, Watanabe K, Hayashi H, Morizane A, Koyanagi M, Sasai Y and Hashimoto N: Fluorescence-activated cell sorting-based purification of embryonic stem cell-derived neural precursors averts tumor formation after transplantation. Stem Cells 24: 763-771, 2006.
30. Lai HC, Lin YW, Huang TH, Yan P, Huang RL, Wang HC, Liu J, Chan MW, Chu TY, Sun CA, Chang CC and Yu MH: Identification of novel DNA methylation markers in cervical cancer. Int J Cancer 123: 161-167, 2008.

ord JM and Barton RW: Thy-1 glycoprotein: structure, ution and ontogeny. Lab Invest 54: 122-135, 1986.
32. Abeysinghe HR, Pollock SJ, Guckert NL, Veyberman Y, Keng P, Halterman M, Federoff HJ, Rosenblatt JP and Wang N: The role of the THY1 gene in human ovarian cancer suppression based on transfection studies. Cancer Genet Cytogenet 149: 1-10, 2004.
33. Lung HL, Bangarusamy DK, Xie D, Cheung AK, Cheng Y, Kumaran MK, Miller L, Liu ET, Guan XY, Sham JS, Fang Y, Li L, Wang N, Protopopov AI, Zabarovsky ER, Tsao SW, Stanbridge EJ and Lung ML: THY1 is a candidate tumour suppressor gene with decreased expression in metastatic nasopharyngeal carcinoma. Oncogene 24: 6525-6532, 2005.
34. Habuchi T, Luscombe M, Elder PA and Knowles MA: Structure and methylation-based silencing of a gene (DBCCR1) within a candidate bladder cancer tumor suppressor region at 9q32-q33. Genomics 48: 277-288, 1998.
35. Gao S, Worm J, Guldberg P, Eiberg H, Krogdahl A, Sørensen JA, Liu CJ, Reibel J and Dabelsteen E: Loss of heterozygosity at 9q33 and hypermethylation of the DBCCR1 gene in oral squamous cell carcinoma. Br J Cancer 91: 760-764, 2004.
36. Izumi H, Inoue J, Yokoi S, Hosoda H, Shibata T, Sunamori M, Hirohashi S, Inazawa J and Imoto I: Frequent silencing of DBC1 is by genetic or epigenetic mechanisms in non-small cell lung cancers. Hum Mol Genet 14: 997-1007, 2005.
37. Maestro R, Dei Tos AP, Hamamori Y, Krasnokutsky S, Sartorelli V, Kedes L, Doglioni C, Beach DH and Hannon GJ: Twist is a potential oncogene that inhibits apoptosis. Genes Dev 13: 2207-2217, 1999.
38. Fackler MJ, McVeigh M, Mehrotra J, Blum MA, Lange J, Lapides A, Garrett E, Argani P and Sukumar S: Quantitative multiplex methylation-specific PCR assay for the detection of promoter hypermethylation in multiple genes in breast cancer. Cancer Res 64: 4442-4452, 2004.